IEEE International Conference on Image Processing (ICIP12), Orlando, FL, Sept. 2012

GRADIENT-BASED SURFACE RECONSTRUCTION USING COMPRESSED SENSING

Mohammad Rostami, Oleg Michailovich, and Zhou Wang

Department of Electrical & Computer Engineering, University of Waterloo, Waterloo, Canada
Email: m2rostami@uwaterloo.ca, olegm@ecemail.uwaterloo.ca, zhouwang@ieee.org

ABSTRACT

Surface reconstruction from measurements of spatial gradient is an important computer vision problem with applications in photometric stereo and shape-from-shading. In the case of morphologically complex surfaces observed in the presence of shadowing and transparency artifacts, a relatively large number of gradient measurements may be required for accurate surface reconstruction. Consequently, due to hardware limitations of image acquisition devices, situations are possible in which the available sampling density might not be sufficiently high to allow for recovery of essential surface details. In this paper, the above problem is resolved by means of derivative compressed sensing (DCS). DCS can be viewed as a modification of the classical compressed sensing (CS), which is particularly suited for reconstructions involving image/surface gradients. We demonstrate that using DCS results in substantial data savings as compared to the standard (dense) sampling, while producing estimates of higher accuracy and smaller variability, as compared to CS-base estimates. The results of this study are further supported by a series of numerical experiments.

***Index Terms*—** Photometric stereo, shape-from-shading, 3-D surface reconstruction, derivative compressed sensing, Poisson equation

1. INTRODUCTION

The notions of photometric stereo (PS) and shape-from-shading (SFS) [1] are standard in computer vision, with their practical applications ranging from video surveillance to surface quality assessment. In both PS and SFS, a 3-D surface of interest is recovered from the measurements of its spatial gradient. In particular, under some reasonable assumptions on the light source and the object reflection properties, the unit normal to such a surface can be calculated from its grey-scale representation. Consequently, the normal can be used to recover its corresponding partial derivatives, followed by reconstructing an approximation of the original surface through the solution of a Poisson equation.

A practical difficulty in implementation of the above-mentioned techniques stems from the necessity to deal with relatively large sets of gradient data. Typically, such *dense* data sets are required to allow for accurate reconstruction of fine surface details, which are often occluded due to shadowing and transparency artifacts. In such cases, improving the acquisition requirements of the hardware in use through reducing the sampling density would unavoidably produce aliasing artifacts. Fortunately, recent advances in computational harmonic analysis offer a means to overcome the above limitation, while allowing for accurately recovering digital signals from their sub-Nyquist measurements. This method - known as compressed sensing (CS) [2,3] - has already revolutionized vast areas of applied sciences, and computer vision in particular [4].

The original CS framework, however, does not incorporate arbitrary *a priori* information on the interrogated signals, apart from their being sparsely representable in a predefined basis. In particular, at the case at hand, it seems to be natural to reconstruct the surface gradient using the fact that the latter forms a potential vector field. When subjected to such side information, the classical CS setup transforms into its specific instance - known as derivative compressed sensing (DCS) [5] - which is in the heart of the present study. Specifically, in this paper, we introduce a novel method for reconstruction of 3-D surfaces from the sub-critical (incomplete) measurements of their spatial gradients. In addition to detailing a computationally efficient algorithm for DCS [6], it is shown how the latter can be used to improve the reconstruction quality of the standard CS [2, 3], while resulting in substantial reduction in sampling density.

2. COMPRESSED SENSING IN GRADIENT FIELD

Compressed sensing (CS) is a mathematical technique [2] which provides a tool for sparse reconstruction of signal sources from their sub-Nyquist measurements. A principal result of the CS theory states that a K-sparse signal $\mathbf{z} \in \mathbb{R}^n$ can be recovered from as few as $m = O(K \log(n/K))$ of its linear measurements $\mathbf{y} \in \mathbb{R}^m$ [2,3], which are assumed to be acquired according to

$$\mathbf{y} = \Psi \mathbf{z} + \mathbf{n}, \tag{1}$$

where $\Psi \in \mathbb{R}^{m \times n}$ denotes a sensing matrix (with $n > m$) and $\mathbf{n}$ is included to account for measurement noise.

Due to the overcompleteness of Ψ, the problem of recovering $\mathbf{z}$ from its noisy measurements $\mathbf{y}$ is ill-posed. However, if Ψ obeys the restricted isometry property (RIP) [2,3] with respect to K-sparse signals, the classical CS framework suggests that a useful approximation of $\mathbf{z}$ can be obtained by solving

$$\mathbf{z} = \arg\min_{\mathbf{z}'} \left\{ \|\mathbf{z}'\|_1 \mid \|\Psi \mathbf{z}' - \mathbf{y}\|_2^2 \le \epsilon \right\}, \tag{2}$$

where $\epsilon > 0$ is a user-defined parameter, which controls the level of noise. Note that the problem (2) is strictly convex, and hence admits a unique minimizer. Several algorithms, using the convex analysis and optimization, have been developed in the literature for solving (2).

Let $z(x, y)$ represent an original surface. For the sake of convenience, $z(x, y)$ is assumed to be defined over a finite-dimensional, uniform, rectangular lattice in $\mathbb{R}^2$, so that its partial derivatives $\mathbf{z}_x$ and $\mathbf{z}_y$ can be concatenated into two column vectors by means of lexicographic ordering. The observed versions $\mathbf{b}_x$ and $\mathbf{b}_y$ of vectors $\mathbf{z}_x$ and $\mathbf{z}_y$, respectively, are obtained as $\mathbf{b}_x = \Psi_x \mathbf{z}_x$ and $\mathbf{b}_y = \Psi_y \mathbf{z}_y$, where Ψ_x and Ψ_y are subsampling matrices which account for the effect of partial observation. Finally, it is also assumed that the partial derivatives $\mathbf{z}_x$ and $\mathbf{z}_y$ admit sparse representations with respect to a linear transformation W, which implies the existence of two (sparse) vectors of representation coefficients $\mathbf{c}_x$ and $\mathbf{c}_y$ such that $\mathbf{z}_x = W\,\mathbf{c}_x$ and $\mathbf{z}_y = W\,\mathbf{c}_y$.

Under the above conditions, CS-based reconstruction of the representation coefficients $\mathbf{c}_x$ and $\mathbf{c}_y$ can be performed according to

$$\mathbf{c}_x^* = \arg\min_{\mathbf{c}'_x} \left\{ \frac{1}{2}\|\Psi_x W \mathbf{c}'_x - \mathbf{b}_x\|_2^2 + \lambda \|\mathbf{c}'_x\|_1 \right\} \tag{3}$$

and

$$\mathbf{c}_y^* = \arg\min_{\mathbf{c}'_y} \left\{ \frac{1}{2}\|\Psi_y W \mathbf{c}'_y - \mathbf{b}_y\|_2^2 + \lambda \|\mathbf{c}'_y\|_1 \right\}. \tag{4}$$

Moreover, by allowing $\mathbf{c} = [\mathbf{c}_x, \mathbf{c}_y]^T$, $\mathbf{b} = [\mathbf{b}_x, \mathbf{b}_y]^T$, and $A = \mathrm{diag}\{\Psi_x W, \Psi_y W\}$, one can solve both (3) and (4) simultaneously as

$$\mathbf{c}^* = \arg\min_{\mathbf{c}'} \left\{ \frac{1}{2}\|A\mathbf{c}' - \mathbf{b}\|_2^2 + \lambda \|\mathbf{c}'\|_1 \right\}. \tag{5}$$

This formulation is equivalent to (2) and hence the CS solver algorithms can be used to handle this optimization problem.

The DCS algorithm of [5] extends the CS approach by using the fact that, for twice differentiable surfaces $z(x, y)$, $\frac{\partial^2 z}{\partial x\,\partial y} = \frac{\partial^2 z}{\partial y\,\partial x}$. This fact can be incorporated as an additional, *cross-derivative* constraint as follows. Let D_x and D_y denote the matrices of discrete partial differences in the direction of x and y, respectively. Then, the cross-derivative constraint suggests that

$$D_x \mathbf{z}_y = D_y \mathbf{z}_x. \tag{6}$$

Consequently, the DCS approach recovers the optimal $\mathbf{c}^*$ as a solution to the following constrained problem

$$\mathbf{c}^* = \arg\min_{\mathbf{c}'} \left\{ \frac{1}{2}\|A\mathbf{c}' - \mathbf{b}\|_2^2 + \lambda \|\mathbf{c}'\|_1 \right\}, \quad \text{s.t. } B\mathbf{c}' = 0 \tag{7}$$

where $B := D_y T_x - D_x T_y$, with T_x and T_y being the operators of coordinate projections, defined as $\mathbf{c}_x = T_x\,\mathbf{c}$ and $\mathbf{c}_y = T_y\,\mathbf{c}$.

A solution to (7) can be found by means of the Bregman algorithm [7], in which case $\mathbf{c}^*$ is computed iteratively as given by

$$\begin{cases} \mathbf{c}^{(t+1)} = \arg\min_{\mathbf{c}'} \left\{ \frac{1}{2}\|A\mathbf{c}' - \mathbf{b}\|_2^2 + \right. \\ \qquad\qquad \left. +\lambda\|\mathbf{c}'\|_1 + \frac{\delta}{2}\|B\mathbf{c}' + p^{(t)}\|_2^2 \right\} \\ p^{(t+1)} = p^{(t)} + \delta B \mathbf{c}^{(t+1)}, \end{cases} \tag{8}$$

where $p^{(t)}$ is a vector of Bregman variables and $\delta > 0$ is a user-defined parameter. Given the optimal solution $\mathbf{c}^*$, the *dense* partial derivatives are recovered as $\mathbf{z}_x = W\,T_x\,\mathbf{c}$ and $\mathbf{z}_y = W\,T_y\,\mathbf{c}$, followed by reconstructing an approximation of the surface z via solution of a Poisson equation [6]. All the proposed algorithmic steps are summarized in Algorithm 1 below.

3. SURFACE RECONSTRUCTION IN GRADIENT FIELD

Gradient space is the 2-D space of all (z_x, z_y) points. It is convenient to represent surface orientation in this space. In practice the gradient field is determined via the reflectance map $R(z_x, x_y)$ [8], which in turn is measured empirically. The reflectance map can be viewed as a 2-D image $i(x, y)$, where the image intensity is a function of z_x and z_y.

Algorithm 1: Derivative Compressive Sampling

1. *Data:* $\mathbf{b}_x, \mathbf{b}_y$, and $\lambda > 0$
2. *Initialization:* For a given transform matrix W and matrices/operators Ψ_x, Ψ_y, D_x, D_y, T_x and T_y, preset the procedures of multiplication by A, A^T, B and B^T.
3. *Gradient field recovery:* Starting with an arbitrary $\mathbf{c}^{(0)}$ and $p^{(0)} = 0$, iterate (8) until convergence to result in an optimal $\mathbf{c}^*$. Use the estimated (full) partial derivatives $WT_x\mathbf{c}^*$ and $WT_y\mathbf{c}^*$ to recover the values of $\mathbf{z}_x$ and $\mathbf{z}_y$.
4. *Source recovery:* Use a Poisson solver to reconstruct the original source from its gradient field

For Lambertian surfaces [8], the light is reflected in a given direction only based on the surface orientation. If the the measuring camera is placed at infinity (a single distant point source), the reflectance map based on Lambertian shading rule is given as [8],

$$R(z_x, z_y) = \frac{\rho(1 + z_x p_s + z_y q_s)}{\sqrt{1 + z_x^2 + z_y^2}\sqrt{1 + p_s^2 + q_y^s}} \tag{9}$$

where ρ is a reflectance factor.

The idea for both PS and SFS is to vary the viewing direction for measuring the x and y components of the gradient field of a surface, $z(x, y)$, at discrete points. Although the surface orientation is fixed, this will affect the reflectance map. For known ρ at least two views are required for determining z_x and z_y. But due to the nonlinearity in (9), more than on solution may exist. To emit such extra solutions, at least three measurements with three different light directions are required to solve uniquely for z_x and z_y. In practice, for improving the measurements, N images $i(x, y) = R(z_x, z_y)$ may be used $(N > 3)$. These images result in the following equation for each point (x_i, x_j),

$$\begin{bmatrix} i_1(j,i) \\ \vdots \\ i_N(j,i) \end{bmatrix} = \begin{bmatrix} d_{1x} & d_{1y} & d_{1z} \\ \vdots & \vdots & \vdots \\ d_{nx} & d_{ny} & d_{nz} \end{bmatrix} \begin{bmatrix} \hat{n}_x \\ \hat{n}_y \\ \hat{n}_z \end{bmatrix} \tag{10}$$

where (d_{kx}, d_{ky}, d_{kz}) is the k^{th} light ray direction and $\hat{\mathbf{n}}^T = [\hat{n}_x, \hat{n}_y, \hat{n}_z]^T$ is the surface normal vector. This equation in matrix form can be written as:

$$I = D\hat{\mathbf{n}}, \tag{11}$$

and the least square solution is given by

$$\hat{\mathbf{n}} = D^+ I, \tag{12}$$

where D^+ denotes Moore pseudo-inverse of D. Having the surface normal vector, the x and y components of the gradient field can be computed: $z_x = \hat{n}_x/\hat{n}_z$ and $z_y = \hat{n}_y/\hat{n}_z$. Consequently, over the whole surface the following measurements are obtained:

$$\begin{aligned} Z_x(j,i) &= \frac{\partial z}{\partial x}\Big|_{(x,y)=(x_i,y_j)} \\ Z_y(j,i) &= \frac{\partial z}{\partial y}\Big|_{(x,y)=(x_i,y_j)} \end{aligned} \tag{13}$$

For accurate surface reconstruction a high sampling density for the gradient field is required [8]. The sampling density is limited by the measuring device and there may be situations in which the sampling

Table 1. Comparisons of surface recovery results

Image	Sphere				Peak-Valley				Ramp-Peak			
SNR (dB)	10	15	20	25	10	15	20	25	10	15	20	25
	MSE comparison											
DS	0.0017	0.0017	0.0017	0.0017	0.0027	0.0013	0.0002	0.0001	0.0443	0.0139	0.0051	0.0033
CS	0.0057	0.0056	0.0055	0.0055	0.0210	0.0114	0.0103	0.0091	0.3773	0.2239	0.1201	0.0786
DCS	0.0022	0.0019	0.0018	0.0017	0.0071	0.0023	0.0006	0.0002	0.2464	0.0633	0.0157	0.0053

density is not sufficient for recovery of the surface details. This limitation may be resolved by applying DCS to this reconstruction problem. Having the partial measurements of matrices Z_x and Z_y, one can obtain vectors $\mathbf{b}_x$ and $\mathbf{b}_y$ via lexicographical column-stacking and use Algorithm 1 to solve for $\mathbf{z}_x$ and $\mathbf{z}_y$. Analogously this is equivalent with increasing the sampling density of the gradient field without improving the hardware device.

In the final stage of Algorithm 1, it is required to solve a Poisson equation to yield the original source (the surface). Several approaches such as least square (LS) [9], algebraic [10], and l_1-minimization [11] have been proposed in the literature for this purpose. We use LS approach [9] in the current study for solving the Poisson equation.

4. EXPERIMENAL RESULTS

Simulated surfaces from [9] were used to assess the performance of the proposed method. The algorithm was tested over three surfaces known as Sphere, Peak-Valley, and Peak-Ramp. The surface lattices size is chosen 64×64, $\delta = 0.5$, and $\lambda = 0.001$. The subsampling matrices Ψ_x and Ψ_y were obtained from an identity matrix I through a random subsampling of its rows by a factor, r, resulting in a required partial sampling ratio. Fore sparse representation basis, W was selected to be a four-level orthogonal wavelet transform using the nearly symmetric wavelets of Daubechies with five vanishing moments.

For the purpose of comparison we have compared our algorithm with standard dense sampling (DS) and classical CS approaches in terms of MSE. The results of this comparison are summarized in Table 1 for different levels of noise and partial sampling ratio of $r = 0.5$ for classical CS and DCS. As expected, one can see that DCS results in substantially lower values of MSE as compared to classical CS, which implies a higher accuracy of surface reconstruction. As expected DS outperforms both methods but the performance of DCS is comparable and confirms the possibility of simplifying the hardware device using our approach without substantial reduction in reconstruction quality. The reconstruction result for Peak-Ramp surface is given in Fig. 1 for $SNR = 20dB$. Visual inspection on images, specially at the surface edges, confirms that DCS provides a result comparable with that of DS reconstruction. As it can be detected CS reconstruction results in smoothed edges in the ramp part of the surface, manifesting severe reduction of high frequency energy, which, by contrast, is well preserved in DCS reconstruction.

In another set of experiment we studied robustness of the proposed method towards noise addition. The cross-derivative constraints exploited by DCS effectively restricts the feasibility region for an optimal solution. Moreover, as explained in [5], the constraint $B\mathbf{c}' = 0$ in (7), can be considered as extra measurements of the sparse source. These measurements are noise free and consequently one can conclude that if we use this constraint, the reconstruction algorithm will become more robust towards the noise power. To investigate the robustness of the proposed algorithms towards measurement noises, its performances has been compared for a range of SNR values (as a measure for noise power) with classical CS. The results of this comparison are summarized in Fig. 2. As expected in both cases the reconstruction quality degrades by decreasing SNR, but this dependency is more critical for classical CS, which results in steeper graph in Fig. 2. This fact represents another advantage of incorporating the cross-derivative constraints in the process of surface recovery.

5. CONCLUSION

In the present paper, the applicability of DCS to the problem of surface reconstruction is studied. To simplify the measuring devices a CS-based approach has been proposed. The proposed method applies CS for surface reconstruction subject to an additional constraint, which stems from the property of a gradient field. Experiments confirm the source estimates by DCS have better quality as compared to the case of classical CS and comparable as to the case of dense sampling. One direction for future work is applying the algorithm in designing the sampling devices for surface reconstruction. Applying the algorithm in the sampling device structure will improve the capability of reconstructing surface details in presence of low density measurements.

6. ACKNOWLEDGEMENT

This work was supported in part by the Natural Sciences and Engineering Research Council of Canada and in part by Ontario Early Researcher Award program, which are gratefully acknowledged.

7. REFERENCES

[1] H. D. Tagare, D. Hemant, and R. J. deFigueiredo, "A theory of photometric stereo for a class of diffuse non-lambertian surfaces," *IEEE Trans. Pattern Anal. Mach. Intell.*, vol. 13, pp. 133–152, 1991.

[2] E. J. Candés, J. Romberg, and T. Tao, "Robust uncertainty principles: exact signal reconstruction from highly incomplete frequency information," *IEEE Trans. Info. Theory*, vol. 52, no. 2, pp. 489–509, 2006.

[3] Y. Tsaig and D. L. Donoho, "Compressed sensing," *IEEE Trans. Inform. Theory*, vol. 52, pp. 1289–1306, 2006.

[4] P. Boufounos, "Compressive sensing for over-the-air ultrasound," in *Proceedings of the IEEE International Conference on Acoustics, Speech, and Signal Processing (ICASSP 2011)*, 2011, pp. 5972–5975.

[5] M. Hosseini and O. Michailovich, "Derivative compressive sampling with application to phase unwrapping," in *Proceedings of EUSIPCO*, Glasgow, UK, August 2009.

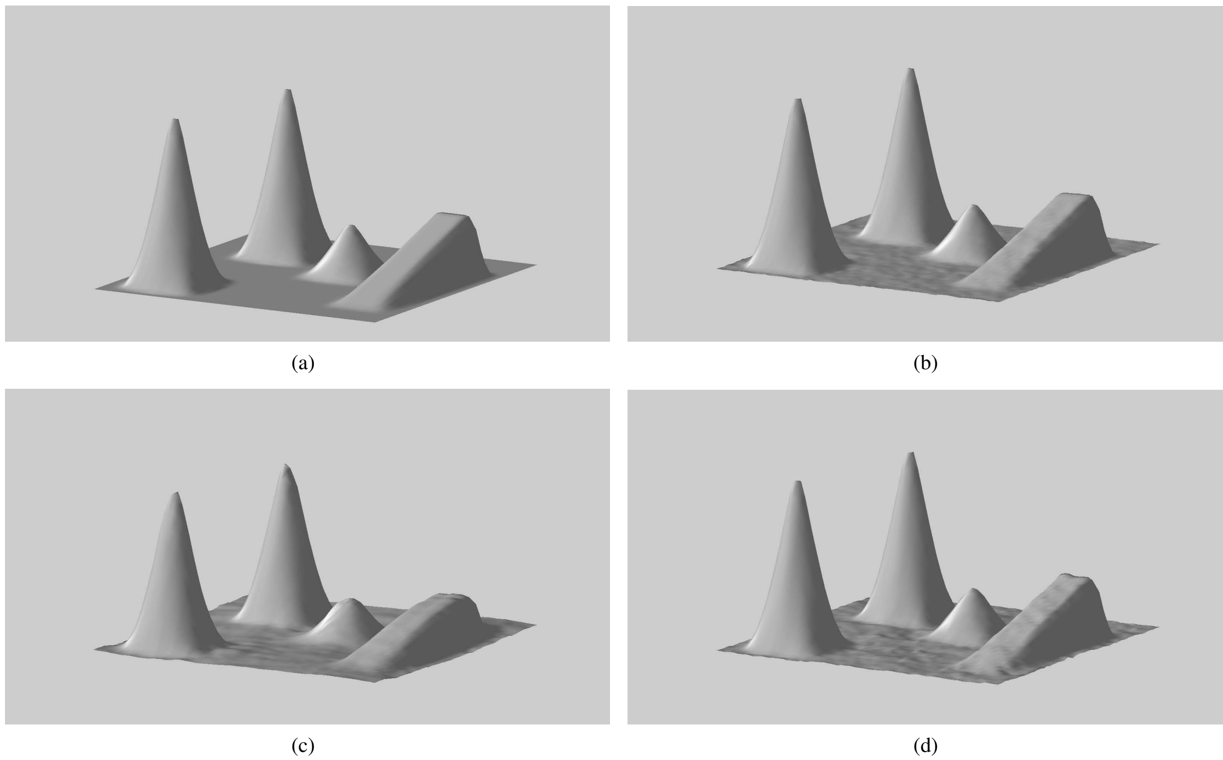

Fig. 1. Peak-Ramp surface (a) and its reconstructed versions using (b) DS, (c) classical CS, and (d)DCS for $SNR = 20dB$.

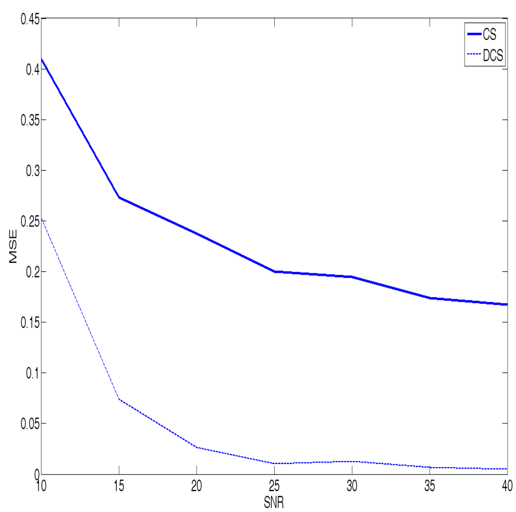

Fig. 2. MSE of surface reconstruction as a function of SNR. Here, the dashed and solid lines correspond to classic CS and DCS, respectively, and $r = 0.5$.

[6] M. Rostami, O. V. Michailovich, and Z. Wang, “Image deblurring using derivative compressed sensing for optical imaging application,” *IEEE Transactions on Image Processing (submitted)*, 2011.

[7] J. Cai, S. Osher, and Z. Shen, “Split bregman methods and frame based image restoration,” *Multiscale Modeling & Simulation*, vol. 8, no. 2, pp. 337–369, 2009.

[8] R. J. Woodham, “Shape from shading,” chapter Photometric method for determining surface orientation from multiple images, pp. 513–531. Cambridge, MA, USA, 1989.

[9] M. Harker and P. O’Leary, “Least squares surface reconstruction from measured gradient fields,” in *The 24th IEEE Conference on Computer Vision and Pattern Recognition (CVPR 2011)*, 2008.

[10] A. Agrawal, R. Chellappa, and R. Raskar, “An algebraic approach to surface reconstruction from gradient fields,” in *Proceedings of the Tenth IEEE International Conference on Computer Vision (ICCV’05)*, 2005, pp. 174–181.

[11] Z. Du and A. Robles-Kelly F. Lu, “Robust surface reconstruction from gradient field using the l1 norm,” in *Proceedings of the 9th Biennial Conference of the Australian Pattern Recognition Society on Digital Image Computing Techniques and Applications (DICTA ’07)*, 2007, pp. 203–209.